Stability of large vacancy clusters in silicon

T.E.M. Staab,[1] A. Sieck,[2] M. Haugk,[2] M.J. Puska,[1] Th. Frauenheim,[2] and H.S. Leipner[3]
[1]*Helsinki University of Technology, Laboratory of Physics, P.O. Box 1100, FIN-02015 HUT, Finland*
[2]*University Paderborn, Department of Physics, Theoretical Physics, D-33098 Paderborn, Germany*
[3]*Martin-Luther-University Halle–Wittenberg, Department of Physics, Friedemann-Bach Platz 6, D-06108 Halle, Germany*
(Received 20 June 2000; revised manuscript received 27 February 2001; published 8 March 2002)

Using a density-functional-based tight-binding method we investigate the stability of various vacancy clusters up to a size of 17 vacancies. Additionally, we compute the positron lifetimes for the most stable structures to compare them to experimental data. A simple bond-counting model is extended to take into account the formation of new bonds. This yields a very good agreement with the explicitly calculated formation energies of the relaxed structures for V_6 to V_{14}. The structures, where the vacancies form closed rings, such as V_6 and V_{10}, are especially stable against dissociation. For these structures, the calculated dissociation energies are in agreement with experimentally determined annealing temperatures and the calculated positron lifetimes are consistent with measurements.

DOI: 10.1103/PhysRevB.65.115210 PACS number(s): 61.72.Ji, 78.70.Bj

I. INTRODUCTION

Vacancy clusters in silicon are detected by electron paramagnetic resonance (EPR), positron annihilation spectroscopy (PAS), and other methods not only after damage (electron[1–4] and neutron irradiation[5–7] or plastic deformation[8]), but also in as-grown samples.[9] Due to a lack of computational data on structure and stability of vacancy clusters detected in silicon in the 1970's and 1980's, their size has been under discussion for a long time. Based on a simple theoretical model, namely, the counting of dangling bonds, it has been proposed[10] that closed ring structures of vacancies, as they occur for V_6 and V_{10}, should be especially stable. This type of simple model is important since it can — without any calculations — give a rough idea about what energetically favorable structures may look like (see also Ref. 11 for results on surface reconstructions and relaxations of zinc-blende semiconductors). But still explicit and accurate calculations on the stability and structure of larger vacancy clusters in silicon and a reasonable comparison to experimental results are rare. Until not long ago, accurate *ab initio* calculations have been performed only for very small structures (mono- and divacancies) due to the limited size of the supercell (64 atoms) used.[12] Using a small supercell with 38 atoms the Hartree-Fock method has been applied to clusters with up to 8 vacancies.[13] Massive parallel computing has made it possible to treat larger supercells, which seem to be necessary to obtain converged results even for mono- and divacancies.[14,15] To our knowledge there exists only one approximative treatment based on quantum mechanics for clusters with more than 8 vacancies.[16]

The self-consistent-charge density-functional-based tight-binding (SCC-DFTB) method[17,18] offers the unique possibility to treat larger structures nearly as accurate as with *ab initio* methods. For clusters consisting of more than ten vacancies one has to consider large supercells of about 500 atoms to avoid interactions between the extended defects and their periodic replica and to allow for an unbiased relaxation.

In contrast to metals it seems to be impossible to determine the monovacancy formation enthalpy for silicon or other semiconductors in thermodynamic equilibrium by standard techniques (differential dilatometry or positron annihilation). Due to their relatively high formation enthalpy, no measurable amount of vacancies is created below the melting temperature in silicon. Therefore, it is not possible to directly compare calculated formation energies for defects in silicon to experimental data. Besides EPR, infrared absorption, deep level transient spectroscopy, and other measurements, experimentally determined positron lifetimes, along with a comparison to calculated lifetimes for different vacancy structures, provide a link between theory and experiment.

Electron irradiation at low temperatures creates a high density of Frenkel pairs (monovacancies and interstitial atoms) far from thermodynamical equilibrium. The monovacancies created lead to an experimentally detected defect-related positron lifetime around 275 ps and become mobile at about 150 K.[19] During this annealing stage the formation of divacancies is observed by a change in the defect-related positron lifetime to the range from 290 to 320 ps. Divacancies have been found to be stable up to a temperature of 550 K. At this temperature the divacancies dissociate and anneal, if the sample was irradiated with a low dose. However, they may form vacancy clusters, if the sample was treated with a higher irradiation dose, i.e., had initially a higher defect density. Considering the formation and growth of vacancy clusters, not only their stability against dissociation via disintegration into monovacancies, is an important criterion. But also the energetics of an ''exchange reaction'' (one vacancy is transferred from one *n*-vacancy cluster to another *n*-vacancy cluster) is important, since largers cluster may start to grow on the expense of smaller ones (Ostwald ripening).

Recent results on positron annihilation in neutron irradiated silicon[7,20] and on high-dose electron irradiated silicon[1,21] give a quite consistent picture on stable vacancy clusters formed during thermal treatment by mobile primary defects: After neutron irradiation, larger vacancy clusters are formed during thermal treatment around 870 K with defect-related positron lifetimes of $\tau_{\mathrm{def}}=420\pm20$ ps (Ref. 7) [430 ± 30 ps (Ref. 20)]. After high-dose electron irradiation,

 ©2002 The American Physical Society

vacancy clusters are found after thermal treatment in the same temperature range (around 870 K) with positron lifetimes of $\tau_{\mathrm{def}}=415\pm20$ ps (Ref. 21) [420 ± 30 ps (Ref. 1)]. In all these cases, annealing of these vacancy clusters takes place at about 1000 K. The errors given are estimated by us according to statistical errors, background and positron source corrections, and difficulties in decomposing the spectra.[22,23]

Considering the experimental results on deformed silicon, the picture emerging from experiments is somewhat different: While EPR indicates the presence of the Si-*P*1 paramagnetic center, significantly higher defect-related positron lifetimes than in irradiated material are found after a similar thermal treatment.[8,24–26] High strain rates and low deformation temperatures (about 800 K) seem to favor much larger vacancy clusters: 590 ± 90 ps (Ref. 8) [600 ± 50 ps (Ref. 26)]. These long lifetimes indicate trapping at surface positron states at the inner surfaces of large vacancy clusters. Lower deformation rates and/or higher deformation temperatures (about 1000 K) lead to significantly smaller defect-related positron lifetimes: $435\cdots480$ ps (Ref. 25) or 485 ± 30 ps (Ref. 26). All defects including vacancy clusters and dislocations are found to anneal out around 1100 K.[8,26]

Experimentally detected defect-related positron lifetimes and, thereby, information on their size have errors of typically 30 ps for larger vacancy clusters ($\tau=400$–500 ps). We shall see that these errors are in the same range as the calculated lifetime differences between, e.g., V_{10} and V_{14}. Hence, the measured defect-related lifetimes cannot uniquely be related to a certain vacancy cluster size by just comparing experiments to positron lifetime calculations.

Since the assignment of defect-related positron lifetimes to certain sizes of vacancy clusters is still under discussion, it is highly desirable to combine information on the stability of vacancy clusters and their respective annihilation parameters. Hence, we have determined the geometries and formation energies of various vacancy clusters in bulk silicon consisting of up to $n=17$ vacancies in a $512-n$ supercell. The investigated structures include vacancy clusters where the atoms have been removed from a hexagonal ring network and chains along $\langle 1\bar{2}1\rangle$ and along $\langle 110\rangle$ with three to six vacancies and some compact vacancy clusters. Chains of vacancies seem to play an important role during the creation of multivacancy clusters by plastic deformation. Additionally, we have calculated the corresponding defect-related positron lifetimes and have compared them to experimental data.

II. METHODS

We have relaxed the structures with the self-consistent-charge density-functional-based tight-binding method[17,18] using a minimum basis set and the Γ-point approximation. The electron density of an extended system described in this method is a superposition of compressed atomic electron densities. Anticipating in this way the results of fully self-consistent-field calculations, only the Mulliken charges are redistributed until the charge distribution is consistent with the charge-dependent energy operator. A pure two-center approach allows for the efficient setup of the Hamiltonian and overlap matrices of the total system and, therefore, for a fast calculation of the total energy and forces. The SCC-DFTB method is proven to yield accurate geometries, energies, and vibrational frequencies for the silicon bulk phases, surfaces, defects, and also for silicon clusters.[17,27] The efficiency of this method implemented on a parallel computer allows for the use of large supercells with $512-n$ atoms.[28] Supercells of at least 216 atoms are expected to be necessary to obtain converged results for the monovacancy.[14] For extended vacancy clusters even larger supercells are needed. This is quite obvious if one compares the size of a $4\times4\times4$ supercell with eight atoms per unit cell (side length 21.7 Å) with the diameter of, e.g., V_{14}, which is about 12 Å. The Si-Si interaction within the DFTB method is negligible for distances greater than 10 Å; therefore, the $4\times4\times4$ atomic supercell should be just large enough for vacancy clusters as large as V_{14}. Additionally, the calculations have been repeated in selected cases for larger supercells containing 1000 atoms minus the vacancies in the cluster. We obtained the following results: For V_1 and V_2, believed to be well described even by a 512-atom supercell, the total energy changes by less than 0.1 eV. For the larger vacancy clusters (V_6, V_{10}, and V_{14}) we found deviation for total energy in precisely the same range. This is indicating that using a 512-atom supercell is appropriate to accommodated such a large cluster. Only for V_{17} was the deviation slightly larger (0.2 eV) which may indicate that the limit for the use of the 512-atom supercell was about to be reached. All structures have been relaxed by a conjugate gradient method until the maximum force on each atom dropped below 0.001 $\mathrm{H}/a_{\mathrm{B}}$. In fact, no simulated annealing has been applied, since the total energy surface can be assumed to be not complicated due the constraints of the surrounding lattice. Hence, we believe that a conjugate gradient relaxation leads into or close to the global minimum.

Positron lifetimes for the perfect lattice and for different vacancy cluster configurations have been calculated using the superimposed-atom model by Puska and Nieminen[29] in the semiconductor approach.[30] The superimposed electron densities form the background potential in which the Schrödinger equation for a positron is solved leading to the positron wave function Ψ_+. The enhancement of the electron density at the positron is taken care of by the Boronski-Nieminen enhancement factor Γ.[31] The annihilation rate λ, the reciprocal of the positron lifetime, is calculated as the overlap of the electron density n^- and the positron density $|\Psi_+(\mathbf{r})|^2$:

$$\lambda\propto\int\Gamma(n^-)n^-(\mathbf{r})|\Psi_+(\mathbf{r})|^2d\mathbf{r}. \tag{1}$$

To obtain accurate positron lifetimes the supercell has to be large enough to avoid interactions between positrons localized at adjacent vacancies of the superlattice. An overlap of the positron wave function with regions of higher electron density in between the defects is known to lead to artificially small lifetimes.

While one finds for silicon mono- and divacancies large inward relaxations, it is assumed that outward lattice relaxations under the influence of the trapped positron cancel out

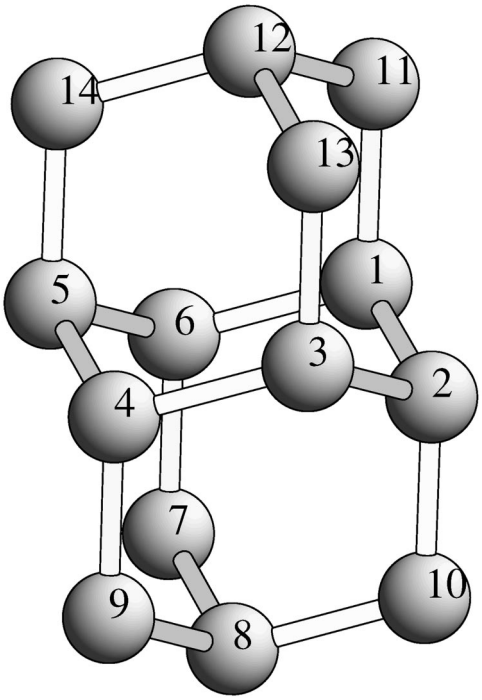

FIG. 1. Atoms were successively removed from this hexagonal ring network starting with atom 1.

or even overcompensate the electronically induced inward relaxations.[32] Because our positron lifetime calculations do not take into account the influence of the trapped positron, we take the positron lifetimes calculated with respect to the unrelaxed geometries to compare them to experimental data.

III. RESULTS

For clusters with more than six vacancies many different configurations are conceivable. To limit the computational effort we focus on candidates, which are likely to have low formation energies because of a small number of dangling bonds. As proposed before,[10] vacancy structures where the removed atoms form closed rings with a minimum number of dangling bonds should be especially stable. For the hexavacancy cluster V_6 this has been confirmed by Hartree-Fock (HF) calculations,[13] where it is found that the hexagonal ring is the most stable of all possible structures. Hence, we have removed the atoms in different ways from the 14-atom cagelike network displayed in Fig. 1, to find the most stable vacancy clusters with up to $n=14$ vacancies. Additionally, we have considered chainlike vacancies in the $\langle 1\bar{2}1\rangle$ direction (direction of jog dragging in deformation experiments) and zigzag chains in the $\langle 110\rangle$ direction with up to six vacancies to provide a comparison to more open vacancy clusters. For V_{10} and V_{17} we have also checked the formation energies of compact vacancy clusters, where the nearest- and some of the next-nearest-neighbor atoms of a vacancy have been removed. For all relaxations we have used a supercell of $N-n(N=512)$ atoms and the lattice constant for the ideal crystal in the DFTB method of 5.43 Å. The atoms around the vacancy have been randomly displaced by a small amount to allow for a symmetry-unrestricted relaxation.

To determine the relative stability of different n-vacancy cluster geometries, we calculate their formation energies

$$E_{\mathrm{F}}^{n}=E_{\mathrm{vac}}^{n}-\frac{N-n}{N}E_{\mathrm{cryst}}^{N}, \tag{2}$$

where E_{vac}^{n} is the total energy of the supercell containing $N-n$ atoms and, hence, an n-vacancy cluster. E_{cryst}^{N} is the total energy of the defect-free supercell of the same size. From this we derive the *dissociation energy*

$$E_{\mathrm{D}}^{n}=(E_{\mathrm{F}}^{n-1}+E_{\mathrm{F}}^{1})-E_{\mathrm{F}}^{n} \tag{3}$$

for the dissociation $V_n \rightarrow V_{n-1}+V_1$ and the *exchange energy*

$$E_{\mathrm{X}}^{n}=(E_{\mathrm{F}}^{n+1}+E_{\mathrm{F}}^{n-1})-2E_{\mathrm{F}}^{n} \tag{4}$$

for the exchange reaction $2V_n \rightarrow V_{n+1}+V_{n-1}$. Provided that only one cluster size is present, the exchange reaction describes, whether a certain cluster size is stable upon that larger ones may grow at the expense of smaller ones (Ostwald-ripening process).

For each vacancy cluster size n up to $n=14$ those structures where one removes the atoms 1 to n from the 14-atom hexagonal ring network displayed in Fig. 1 have the lowest formation energies. The formation and dissociation energies of these structures calculated within the SCC-DFTB method are summarized in Table I and Fig. 2. For comparison the same energies as calculated with an empirical tight-binding method[16] are given in Table I as well. Furthermore, for vacancy sizes up to V_7 the dissociation energies E_{D}^{n} obtained for the same configurations with a Hartree-Fock method are included.[13]

Comparing the formation energies between the SCC-DFTB and empirical TB methods one notices that the overall trend with increasing cluster size is very similar. However, there are important deviations in the differences of the formation energies of one vacancy cluster size compared to the next larger size. This results in a different order in the dissociation energies. The SCC-DFTB method predicts V_6, V_{10}, and V_{14} to have high dissociation energies, whereas the empirical TB method predicts maximum dissociation energies for V_6, V_8, V_{12}, and V_{16}. The SCC-DFTB dissociation energies agree much better with the corresponding HF energies. Only for V_3 is the deviation of the SCC-DFTB value compared to the HF value as large as within the empirical TB method. But the reliability of the HF values may suffer from the quite small supercell used. Hence, the SCC-DFTB method seems to be the method of choice, giving us the opportunity to do calculations in large supercell nearly as exact as *ab initio* methods. Also the maxima in the SCC-DFTB dissociation energies for V_6, V_{10}, and V_{14} are in agreement with the dangling-bond counting model.[10]

Additionally, we have considered configurations of vacancy clusters, where different atoms have been removed from the 14-atom hexagonal ring network displayed in Fig. 1 and we find the formation energies of them to be higher in energy (see Table II). One exception is V_8, where atoms 1, 2, 4–6 and 8–10 in Fig. 1 have been removed. This single-ring

TABLE I. Formation energies E_F^n of different n-vacancy clusters as calculated within the DFTB and empirical TB methods and dissociation energies E_D^n within DFTB, HF, and empirical TB methods. Columns 2–5 correspond to the simple and extended bond-counting models. The numbers of broken and new bonds are given by n_b and n_n, respectively.

	Bond-counting models					Quantum-mechanical methods				
			Simple	Extended	TB [a]	——DFTB——			HF [b]	TB [a]
n	n_b	n_n	E_F^n (eV)	E_F^n (eV)	E_F^n (eV)	E_F^n (eV)	E_X^n (eV)	E_D^n (eV)	E_D^n (eV)	E_D^n (eV)
1	4	2	5.6	3.4	3.4	3.8	−1.8	0.0	0.0	0.0
2	7	4	8.4	3.9	5.2	5.8	0.2	1.8	1.7	1.6
3	10	5	11.2	5.6	7.1	8.0	−0.8	1.6	2.1	1.5
4	13	6	14.0	7.3	9.4	9.4	−0.6	2.4	1.9	1.2
5	16	7	16.8	9.0	10.7	10.1	−0.4	3.1	3.1	2.1
6	18	6	16.8	10.0	11.4	10.5	2.1	3.5	3.8	2.7
7	21	6	19.6	12.9	13.7	12.9	−0.8	1.4	1.3	1.1
8	24	7	22.4	14.6	14.1	14.5	−1.3	2.2	—	3.0
9	26	7	22.4	14.6	14.7	14.8	0.1	3.5	—	2.8
10	28	6	22.4	15.7	15.6	15.2	2.5	3.4	—	2.6
11	31	6	25.2	18.5	17.8	18.2	−1.7	0.8	—	1.2
12	34	7	28.0	20.2	18.3	19.5	−0.3	2.5	—	3.0
13	36	7	28.0	20.2	18.9	20.5	−0.3	2.8	—	2.8
14	38	6	28.0	21.3	19.6	21.2	0.9	3.1	—	2.7
15	41	6	30.8	24.1	22.0	22.8	−0.5	2.2	—	1.0
16	44	7	33.6	25.8	22.4	24.0	0.0	2.6	—	3.0
17	46	7	33.6	25.8	23.0	25.1	−0.7	2.7	—	2.8
18	48	6	33.6	26.9	23.8	25.6	—	3.3	—	2.7

[a]Reference 16.
[b]Reference 13.

structure also exhibits a low number of dangling bonds and, therefore, has about the same energy as V_8 with atoms 1–8 in Fig. 1 removed. It might be interesting to note that V_{12} (atoms 1–6, 8–12, and 14 removed) is the double hexavacancy ring which is a very stable vacancy cluster in GaAs.[33]

Within the SCC-DFTB method, the chainlike vacancies in the $\langle 1\bar{2}1 \rangle$ direction have significantly higher formation energies than vacancy clusters of the same size taken from the hexagonal ring. Because the even-numbered types of these chainlike vacancies consist of ''isolated'' nearest-neighbor vacancy pairs, their formation energies are roughly multiplies of the formation energy of the divacancy (5.8 eV). The formation energies for the ''zigzag'' chains along $\langle 110 \rangle$ for V_4–V_6 are higher compared to the vacancy clusters of the same size taken from the hexagonal ring. Additionally, we have calculated the energies of two *compact* vacancy clusters, namely, a compact V_{10}, where we have removed one atom along with its four nearest neighbors plus five of the next-nearest neighbors, and a compact V_{17}, where we have removed one atom along with its four nearest neighbors and all 12 next-nearest neighbors. The formation energy of the compact V_{10} structure is higher by 2.8 eV compared to the adamantine cage V_{10}. But the compact V_{17} structure exhibits a lower formation energy than the V_{17} structure, where one removes all 14 atoms displayed in Fig. 1 along with three atoms from an adjacent hexagonal ring. All formation energies of the vacancy clusters different from the structures where one removes atoms 1–n in Fig. 1 are summarized in Table II. Our tight-binding calculations suggest that for all sizes up to V_{14} the vacancy clusters indicated in Fig. 1 are the most stable. For vacancy clusters larger than V_{16}, the more compact structures become competitive in energy due to a higher flexibility in the relaxation pattern compared to the ring structures. The transition from the construction model for hexagonal rings to the compact spherical growth pattern is predicted by the SCC-DFTB method for a smaller vacancy cluster size than by the empirical TB method in Ref. 16. There, the compact spherical-shaped V_{24} was found to be the smallest vacancy cluster having a formation energy below the hexagonal ring cluster of the same size.

For the smaller vacancy defects there exist results obtained with more sophisticated *ab initio* methods, to which we can compare our tight-binding results:

In silicon, the monovacancy with T_d symmetry is Jahn-Teller instable and distorts into D_{2d} symmetry. We calculate for the latter symmetry a formation energy of $E_F^1 = 3.8$ eV, which is in reasonable agreement with other first-principles calculations [3.27 eV (Ref. 14), 3.49 eV (Ref. 34), and 3.29 eV (Ref. 12)]. The symmetry breaking results in two different nearest-neighbor distances between the four atoms surrounding the vacancy. The relaxation with the SCC-DFTB method yields distances of 2.8 Å and 3.0 Å, while Antonelli *et al.*[34] find two slightly distinct distortions with identical formation energies. They have calculated the distances to be 3.0 Å and 3.5 Å for their structure *A* and 3.4 Å and 3.5 Å for their structure *B*. Puska *et al.* find with a 216-atom

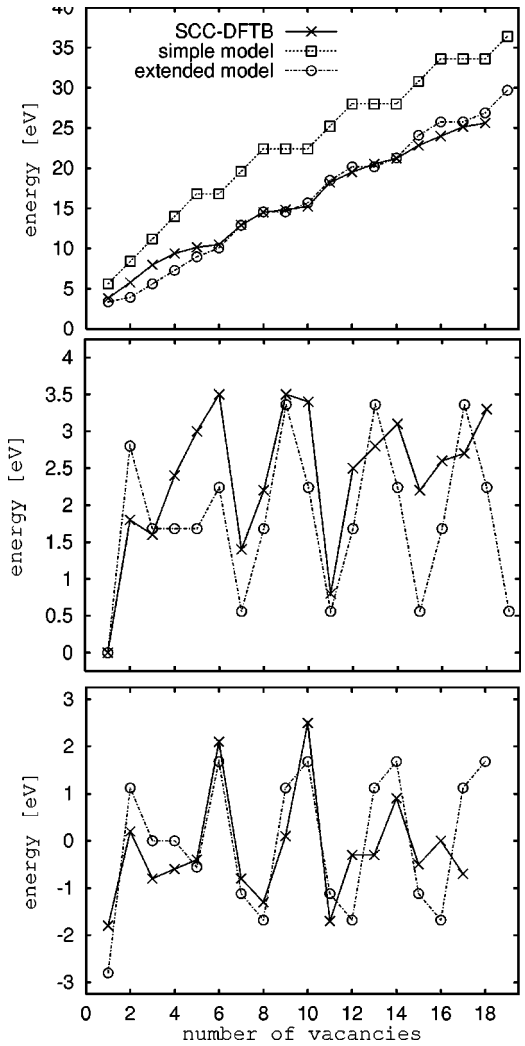

FIG. 2. (Top) Formation energies in eV as a function of the number of vacancies calculated within the SCC-DFTB method, the simple bond-counting model, and the extended bond-counting model (see text). (Middle) Energies in eV for the dissociation $V_n \rightarrow V_{n-1}+V_1$ within the DFTB and the extended bond-counting models. (Bottom) Energies in eV for the exchange reaction $2\,V_n \rightarrow V_{n+1}+V_{n-1}$ within the DFTB and the extended bond-counting models.

supercell using the Γ point and a pseudopotential plane-wave code 2.9 Å and 3.4 Å .[14] The calculations indicate a very flat potential in the direction of the distortion, which makes it difficult to determine the exact equilibrium distances. The nearest-neighbor distance in bulk silicon is 2.35 Å.

Taking two nearest-neighbor atoms away from the ideal crystal yields a Jahn-Teller instable D_{3d} configuration for V_2, which distorts within the DFTB method into C_{2h} symmetry, corresponding to the resonant-bond configuration in Ref. 15. The three nearest neighbors of each of the two removed atoms built an isosceles triangle with two edges of 2.8 Å and one edge of 3.4 Å. In the undistorted crystal these three atoms built an equilateral triangle with an edge length of 3.8 Å, the next-nearest-neighbor distance. During the relaxation, the two triangles shorten their distance by about 0.3 Å. That means that there is an inward relaxation and the volume of the divacancy is reduced. A recent result with a plane-wave pseudopotential approach and a 216-atom supercell gives $E_F^2=4.94$ eV and a binding energy of $E_D^2=1.6$ eV ,[35,36] close to the DFTB result of 1.8 eV. We obtain a formation energy of $E_F^2=5.8$ eV for the divacancy. This value is very close to the 5.7 eV found by Song *et al.*with a TB approach,[37] but deviates by more than 1 eV from the 4.3 eV calculated by Seong and Lewis[12] with a first-principles DFT local density approximation (LDA) plane-wave code. However, they stated that their results fully converged with respect neither to the basis set nor to the size of the supercell.

Comparing the stability between vacancy clusters of different sizes, we find V_6 and V_{10} having ''surfaces'' consisting of adjacent closed vacancy hexagonal rings (see Figs. 3 and 4) to be especially stable. Both vacancy clusters have low relative formation energies (compared to the next larger vacancy cluster as shown in Fig. 2) and a high stability against dissociation into $V_{n-1}+V_1$ and against the exchange reaction $2V_n \rightarrow V_{n+1}+V_{n-1}$ (see Fig. 2). For V_{10} this is in agreement with more qualitative predictions[10] and for V_6 additionally with other calculations.[13] With respect to E_D also V_9, V_{13}, and V_{14} are especially stable.

In the supercell with the hexagonal ring vacancy cluster V_6, each two atoms sitting next to a vacancy site shorten their distance during relaxation from 3.8 Å, the next-nearest-neighbor distance in the ideal crystal, to 2.7 Å. Assuming distances less than 2.8 Å as bonds, all atoms in this relaxed vacancy cluster are fourfold coordinated [cf. Fig. 3(b)]. The bond angles, ranging from 98° to 145°, however, deviate substantially from the tetrahedral bond angle of 109°. In total, six new bonds for the hexavacancy cluster are formed (see Fig. 3).

The nearest-neighbor arrangement is different in the V_{10} vacancy cluster, the adamantine cage (see Fig. 4). Here, four atoms have, in addition to one neighboring vacancy site, three empty next-nearest-neighbor sites and remain, therefore, threefold coordinated after the relaxation [see Fig. 4(b)]. Similar to the case of the hexagonal ring vacancy cluster, the other atoms around the vacancy cluster build new bonds (2.65 Å long) to a next-nearest neighbor (cf. Fig. 4). For V_{10} the total number of new bonds formed is 6, not more than for V_6. The formation of one of these six new bonds in V_{10} is illustrated in Fig. 5. The particle density between the two atoms is significantly increased compared to the density between two next-nearest neighbors in the ideal crystal, but not as high as between two nearest neighbors in the ideal crystal.

In the cagelike V_{14} vacancy cluster there are eight vacancy sites with three nearest-neighbor vacancy sites and, therefore, this vacancy cluster has eight only threefold-coordinated atoms [cf. Fig. 6(b)]. Here, again the total number of new bonds formed does not exceed 6, and is the same as for V_6 and V_{10}.

To allow for a direct comparison to experimental data, we additionally have calculated the defect-related positron lifetimes — given in Table III and Fig. 7. We include for comparison, besides the positron lifetimes calculated with respect

TABLE II. Formation energies obtained with the SCC-DFTB method for vacancy clusters not following the straightforward construction scheme of the hexagonal ring network. The numbers in the third column refer to Fig. 1. The vacancy clusters denoted *compact* consist of one vacancy plus four nearest-neighbor vacancies plus 5 next-nearest neighbor vacancies (V_{10}) and of one vacancy plus four nearest-neighbor vacancies plus 12 next-nearest-neighbor vacancies (V_{17}).

Vacancy cluster	Remark	Atoms removed	E_F^n(eV)	E_D^n	E_F^n(eV) (ext. model)
V_3	$\langle 110\rangle$ chain		8.0	1.6	
V_4	$\langle 110\rangle$ chain		9.2	2.6	7.3
V_5	$\langle 110\rangle$ chain		11.5	1.5	9.0
V_6	$\langle 110\rangle$ chain		13.0	2.3	10.6
V_3	$\langle 1\bar{2}1\rangle$ chain		9.4	0.2	
V_4	$\langle 1\bar{2}1\rangle$ chain		11.5	1.7	7.8
V_5	$\langle 1\bar{2}1\rangle$ chain		15.0	0.3	11.2
V_6	$\langle 1\bar{2}1\rangle$ chain		17.0	1.8	15.6
V_5	Lee and Corbett[a]	[2–4,12,13]	11.5		
V_8	single-ring	[1,2,4–6,8–10]	14.5		13.4
V_8	hexa-ring + 2	[1–6,10,14]	15.4		*
V_9		[1–6,9,10,14]	16.7		*
V_9		[1–6,7,9,10]	15.6		*
V_{10}		[1–6,9-11,14]	19.6		*
V_{10}	compact		18.0		*
V_{12}		[1–6,8–12,14]	20.0		*
V_{12}		[1–10,11,13]	20.4		*
V_{13}		[1–11,13,14]	21.5		*
V_{17}	compact		24.8		*

[a]Reference 6

to the unrelaxed atomic positions, also the lifetimes calculated with respect to the coordinates after relaxation determined by the SCC-DFTB method. As outlined above, the calculated lifetimes obtained from the unrelaxed geometries should better match the measured lifetimes.

The positron lifetimes in Fig. 7 have been calculated using the relaxed and unrelaxed coordinates. The lifetimes increase with increasing cluster size, since the electron density decreases at the location of the vacancy cluster where the positron is trapped. For larger vacancy agglomerations the influence of the trapped positron should decrease, but as shown in Table III and Fig. 7, also the influence of the inward lattice relaxation without positron decreases. Because the potential around the equilibrium geometry is in general very flat for silicon, we expect even for large clusters like V_{14} or V_{17} an influence of the trapped positron pushing the ions slightly outward and, therefore, a better agreement with experimental data for the lifetimes obtained from the unrelaxed structures. Indeed this has been confirmed recently.[38] The main results in this article are that positron-induced

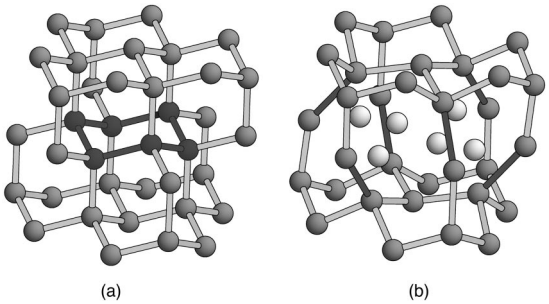

FIG. 3. Black atoms and bonds represent the removed atoms forming a hexagonal ring of V_6 in the ideal crystal (a). In (b) the relaxed atoms around V_6 are shown. White spheres represent the positions of the removed atoms. The six new bonds formed in the relaxed structure are drawn in black. No threefold-coordinated atoms are found in this structure. Further atoms of the surrounding crystal are not shown.

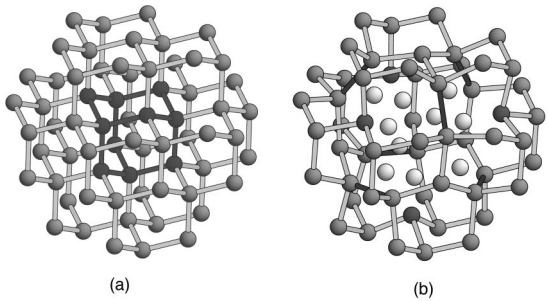

FIG. 4. Black atoms and bonds represent the removed atoms forming a cage of V_{10} in the ideal crystal (a). In (b) the relaxed atoms around V_{10} are shown. White spheres represent the positions of the removed atoms. The six new bonds formed in the relaxed structure are drawn in black. Four threefold-coordinated atoms found in this structure are displayed darker than the others. Further atoms of the surrounding crystal are not shown.

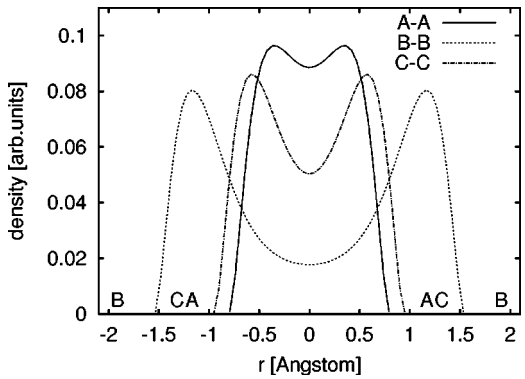

FIG. 5. Electron density along the bond axis. $A-A$ denotes two nearest-neighbor atoms (distance 2.35 Å) and $B-B$ denotes two next-nearest-neighbor atoms (distance 3.8 Å) in the ideal crystal. $C-C$ denotes two atoms in V_{10}, which were next-nearest neighbors in the ideal crystal, but shortened their distance to 2.65 Å during relaxation. The positions of the atoms A,B, and C are indicated on the lower border. Only the central density in between two nodes is shown.

forces nearly balance the electronic forces calculated by the SCC-DFTB method. But we know from a comparison to an *ab initio* plane-wave pseudopotential code for the isolated monovacancy that the SCC-DFTB method overestimates slightly the forces directed inward.[38] Hence, there are strong indications that the net movement of the atoms surrounding a vacancy cluster will hardly differ much from their ideal positions or even may be directed slightly outward. The differences between SCC-DFTB and *ab initio* results may arise from the very flat energy landscape in the case of silicon. We obtain for the most stable vacancy clusters the positron lifetimes $\tau_{V_6}=375$ ps, $\tau_{V_{10}}=420$ ps, and $\tau_{V_{14}}=435$ ps (see Fig. 7 and Table III). The positron lifetime for vacancy chains is even for longer chains very close to the value obtained for divacancies (chains along $\langle 1\bar{2}1\rangle$) or close to that for τ_{V_3} (chains along $\langle 110\rangle$) (cf. Fig. 7).

IV. DISCUSSION

Some results from the tight-binding calculations can be better understood within a *simple bond-counting model*,

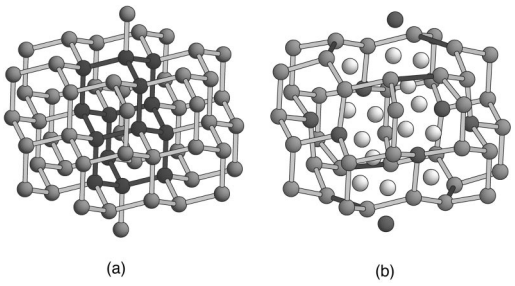

FIG. 6. Black atoms and bonds represent the removed atoms forming a cage of V_{14} in the ideal crystal (a). In (b) the relaxed atoms around V_{14} are shown. White spheres represent the positions of the removed atoms. The six new bonds formed in the relaxed structure are drawn in black. The eight threefold-coordinated atoms found in this structure are displayed darker than the others. Further atoms of the surrounding crystal are not shown.

TABLE III. The defect related positron lifetimes have been calculated for the unrelaxed and the relaxed structures (using the geometry of the DFTB results including only electronic forces). For comparison the known experimental values and those calculated with an alternative method (full relaxed: electronic and positronic forces) are provided for the smaller vacancy clusters.

	Positron lifetime			
	Exp. [a]	No rel. (this work)	Relaxed (this work DFTB)	Full rel. [b]
n	τ(ps)	τ(ps)	τ(ps)	τ(ps)
Bulk	218	218		215
1	282	253	218	279
2	310	303	240	309
3		329	278	320
4		343	291	337
5		353	301	345
6		375	317	348
7		383	330	
8		389	364	
9		398	368	
10		420	385	
11		422	392	
12		425	402	
13		427	406	
14		435	414	

[a]Reference 4
[b]Reference 32

where the cohesive energy of the system simply equals the number of bonds times E_b, the energy per bond in the ideal crystal; i.e., relaxation is neglected. This corresponds to the approach applied in Ref. 10, where it was suggested that the closed hexagonal ring networks (V_6,V_{10}, and V_{14}) should be especially stable due to a relatively low number of dangling bonds. With knowledge about the relaxed structures from our tight-binding calculations one can slightly extend this simple model by taking into account the energy gained by the formation of new bonds. In this *extended bond-counting model* the cohesive energy compared to the simple bond-counting model is lower by the number of new bonds times the average energy per new bond. Generally, for those vacancy positions where the removed atom has had at least two bonds to the surrounding crystal (and not to another vacancy site) a new bond is formed between two atoms in the surrounding crystal, whereas for those vacancy positions where the removed atom has had only one bond to the surrounding crystal (and three to other vacancy sites) a dangling bond is created. The number of broken bonds, n_b, and new bonds, n_n, and the formation energies estimated within the simple and extended bond-counting models for the cases where the atoms have been successively removed from the hexagonal ring network with 14 vacancies (Fig. 1) are given in Table I. Here we use $E_\mathrm{b}=2.8$ eV per bond, the binding energy per bond in the ideal crystal within the SCC-DFTB method. We set the average energy for a new bond to $0.4E_\mathrm{b}$. This value yields formation energies similar to those calculated within the SCC-DFTB method. The details of the simple and of the

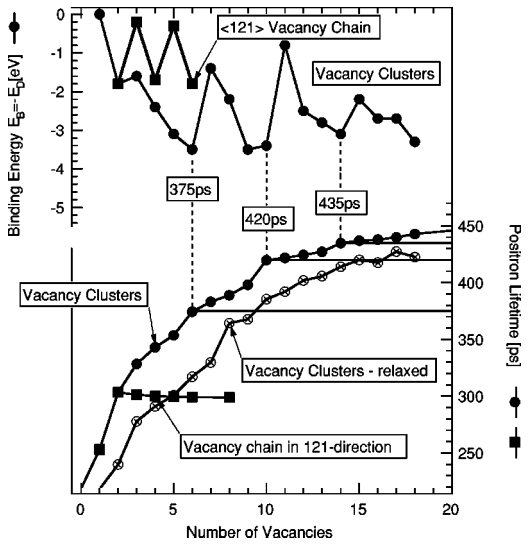

FIG. 7. Binding energy $E_B^n=-E_D^n$ necessary to remove a monovacancy from an agglomeration of n vacancies in silicon (upper part) and the corresponding positron lifetime (lower part) for relaxed and unrelaxed structures. Theoretical positron lifetimes for the most stable structures V_6,V_{10}, and V_{14} are indicated (unrelaxed).

extended bond-counting model can be found in the Appendix.

By comparing the formation and dissociation energies as a function of n as calculated within the DFTB method to those estimates from the extended bond-counting model (Fig. 2), one notices that the extended bond-counting model reproduces the formation energy of the DFTB method as a function of vacancy size n very accurately in the range $6 \leqslant n \leqslant 14$. Furthermore, this model yields local maxima in E_D^n at $n=2,6,9,13$ and local maxima in E_X^n at $n=2,6,10$, in agreement with the tight-binding calculations. However, the simple and extended bond counting models are less predictive for very small and for larger vacancy clusters, where the bonding scheme is more complex. The energy differences for different vacancy structures of the same size predicted by the extended bond-counting model deviate from the calculated energy differences in some cases. Within this model, the formation energies for the ''zigzag'' chainlike vacancies along $\langle 110 \rangle$ V_4 and V_5 are the same as for the vacancy clusters of the same size defined by Fig. 1, whereas the SCC-DFTB calculations yield significantly lower energies for the latter structures. Also the single-ring vacancy structure V_8 (atoms 1,2,4–6, and 8–10 in Fig. 1 removed) is favored by the extended bond-counting model, whereas the SCC-DFTB calculations yield the same formation energies for this structure and V_8 where atoms 1–8 in Fig. 1 have been removed.

Discussing irradiation experiments, not only a low formation and a high dissociation energy of certain cluster sizes are a sufficient criterion for their formation and stability, but also the kinetics of the primary defects becoming mobile during thermal treatment of irradiated samples has to be taken into account. The most important point is the relation between the primary defect density (mainly monovacancies) and the density of sinks for mobile defects. Typical sinks in irradiated Czochralski-grown silicon are oxygen-related microdefects. Hence, there is a always competition between annealing and agglomeration.

A recent work about the defect-related positron lifetime in monovacancies gives $\tau_{V_1}=(282\pm5)$ ps and that monovacancies become mobile at 170 K.[4] The temperature range for the dissociation of divacancies has been determined to be around 550 K. This corresponds to the SCC-DFTB result of a divacancy dissociation energy of 1.8 eV. The activation energy for the migration of monovacancies according to an empirical TB result is estimated to be 1.54 eV.[16] We make the following assumptions to compare experimentally determined annealing temperatures of defects and the corresponding calculated dissociation energies for different clusters: (i) The same barrier height for the diffusion of vacancies away from a cluster, (ii) the same entropy prefactors in the Arrhenius term, and (iii) a similar number of jumps to the nearest sink. We then scale the calculated dissociation energies to that of the divacancy (1.8 eV), which is experimentally well characterized and known to anneal at 550 K. The above-presented three basic assumptions concerning the diffusion of vacancies and the dissolution of vacancy cluster are, to our mind, the most simplest ones possible and may, therefore, be the starting point for a more precise investigation

During thermal treatment of irradiated samples between 550 and 1000 K, the formation of vacancy clusters larger than V_2 is observed by EPR and PAS. Dissociating divacancies seem to form larger vacancy clusters: V_4 is detected by EPR in the temperature range 573–623 K, while the Si-*P*1 EPR center — associated in Ref. 6 to the nonplanar pentavacancy V_5 — is detected for $T=620$–720 K .[5,6] In the same temperature range, the defect-related positron lifetime is rising from $\tau_{\mathrm{def}}\approx310$ ps to values $\tau_{\mathrm{def}}\approx330$–$350$ ps .[2,20,21] This would correspond to V_4 or V_5 defects.

When the Si-*P*1 EPR center is no more detectable ($T>720$ K), PAS detects a value of $\tau_{\mathrm{def}}\approx360$ ps.[20,21] This signal could be due to the V_6 vacancy ring, which probably is invisible by EPR and most other methods, because it exists most likely in the neutral charge state (see also Refs. 13 and 39). For a sufficiently high defect density, τ_{def} keeps on rising with temperature until a saturation value of $\tau_{\mathrm{def}}\approx420$–$430$ is reached at about $T=870$ K.[20,21] There are recent first-principles calculations on defect-related positron lifetimes for several sizes of vacancy clusters in silicon ,[32,40,41] which give positron lifetimes not larger than 360 ps related to trapping into vacancy clusters with five or less vacancies. Our and other calculated positron lifetimes for the unrelaxed structures give 375 ps for V_6, 420 ps for V_{10}, and 435 ps for V_{14}. Combining this information with results on the stability of the vacancy clusters (this work and others[10,13]), one clearly sees that the larger stable clusters are good candidates for the defects related to a positron lifetime of about 430 ps, measured in irradiated silicon annealed up to $T=870$ K. While V_{10} may be formed, it is more unlikely for V_{14}, due to the small dissociation energy $V_{11}\rightarrow V_{10}+V_1$.

Under the assumptions (i)–(iii) made above, the dissociation energies for V_6,V_9, and V_{10} would correspond to annealing at about 1000 K — indeed very close to the experi-

mentally detected annealing temperatures of larger vacancy clusters (420–430 ps).[2,20,21]

It is interesting to note that for medium dose electron irradiation (1×10^{19} cm^{-2} at 6 MeV) the experimentally found defect related positron lifetime is $\approx$350 ps[2] and, hence, is close to the lifetime calculated for V_6.

V. CONCLUSIONS

By calculating the formation energies of various vacancy clusters with up to 17 vacancies with the same density-functional-based tight-binding method in a large supercell along with positron lifetimes for the most stable structures, we are able to limit the number of candidates for stable vacancy clusters in silicon.

We confirm earlier results that the V_6 hexagonal ring and the V_{10} adamantine cage are especially stable.[10,13] Both structures have a low formation energy per vacancy and are also stable against dissociation $V_n \rightarrow V_{n-1}+V_1$ and the exchange reaction $2V_n \rightarrow V_{n+1}+V_{n-1}$. This can be qualitatively understood also in terms of a bond-counting model. However, for large vacancy clusters relaxation effects become more important and sophisticated explicit calculations are indispensable.

The hexagonal ring V_6 and the adamantine cage V_{10} as well as V_{14} vacancy clusters — build from adjacent hexagonal rings — have minimum numbers of dangling bonds in the relaxed structure. All atoms surrounding the V_6 vacancy cluster are fourfold coordinated, while in the V_{10} admantine cage structure four atoms remain threefold coordinated and V_{14} has eight only threefold coordinated atoms. Nevertheless, V_{10} is as stable as V_6, since the energy increase by the threefold-coordinated atoms is compensated by the new bonds formed being closer to the ideal lattice bond length. On the other hand, this effect has not much influence on even larger vacancy clusters ($n>15$), where for the — by the simple bond-counting model predicted — stable structures ($V_{18}, V_{22}, \ldots$) the relative stability is expected to be weakened according to the large number of threefold-coordinated atoms introducing additional dangling bonds. The lower formation energy of the compact V_{17} compared to the vacancy hexagonal ring structure V_{17} indicates that for the larger vacancy clusters these hexagonal ring structures are probably not the most stable ones.

Comparing the dominating vacancy related defect after high-dose irradiation and thermal treatment up to 870 K with the calculated positron lifetimes for the unrelaxed structures V_6(375 ps), V_9(398 ps), V_{10}(420 ps), and V_{14}(435 ps) to the experimentally observed defect-related positron lifetimes of 415–430 ps with errors of roughly 30 ps, we can certainly rule out V_6. Only moderate-dose electron irradiation followed by thermal treatment up to 650 K seems possibly to lead to V_6.

Therefore, we are inclined to believe that V_9 and V_{10} vacancy clusters are the dominating defects determined experimentally in the temperature range $T\approx$870–1000 K. It becomes increasingly difficult to form even larger vacancy clusters like V_{14}, because, on the one hand, the probability of agglomeration decreases with the size of the cluster and, on the other hand, V_{11} is quite unstable against dissociation.

Together with the experimental data, our results agree best with an Ising-like binding model proposed in lattice kinetic Monte Carlo simulations.[42] On the other hand, the extended Ising model,[42] including additionally screened nearest-neighbor interactions, proposes a broad size distribution of vacancy clusters, independent of the initial density of monovacancies, and the annealing temperature. This neither fits the experimental findings, favoring a certain cluster size for given initial defect densities, nor our results, proposing the stability of certain cluster sizes.

ACKNOWLEDGMENTS

We would like to thank Professor R. M. Nieminen (Helsinki University of Technology) and Professor H. Overhof (University of Paderborn) for many interesting discussions. This work was supported by the European Union through a Marie-Curie research grant (T.E.M.S.) and by the Deutsche Forschungsgemeinschaft (A.S.). We also acknowledge the generous computing resources provided by the Center of Scientific Computing (CSC), Espoo, Finland.

APPENDIX: THE SIMPLE AND THE EXTENDED BOND-COUNTING MODEL

In this appendix we outline the details of the simple and the extended bond-counting model. We do this by discussing the breaking and formation of bonds during the creation of vacancies. In the simple bond-counting model, where one does not take relaxation into account, the cohesive energy of the system corresponds to the number of bonds, times the energy per bond, E_b. The ideal crystal with N atoms in the supercell has an energy of $E^N_{\rm cryst}=2\,N\,E_b$. Whereas a n-vacancy cluster with n_b broken bonds has an energy of $E^n_{\rm vac}=(2\,N-n_b)\,E_b$. Therefore, one obtains for the formation energy

$$E^F_n=E^n_{\rm vac}-\frac{N-n}{N}E^N_{\rm cryst}=(2n-n_b)E_b. \tag{A1}$$

For the monovacancy the number of broken bonds n_b equals 4. In the simple divacancy this number equals 7. Removing further atoms on a nearest-neighbor site breaks three additional bonds each time as long as the ''vacancy chain'' remains open. The way how n_b is increasing changes if the removing of a further atom leads to a ''vacancy ring.'' The smallest possible ring consists of six vacancies. Closing the ring changes n_b from 16 for V_5 to 18 for V_6 [see Fig. 3(a)]. Adding a vacancy close to the ring breaks three additional bonds until a second ring is closed. Looking at Fig. 1 one notices that for V_9, where the atoms 1–9 are removed, a second vacancy ring is closed. A third vacancy ring is closed for V_{10} created from V_9 by removing atom number 10. Therefore, the number of broken bonds increases by 2 only if one goes from V_8 to V_9 and from V_9 to V_{10} (see Table I).

One can slightly extend this simple model by considering the energy gained by the formation of n_n new bonds. As described above the four atoms surrounding the monovacancy approximate each other during the relaxation such that

two short distances of 2.8 Å and four slightly larger distances of 3.0 Å occur between the four atoms. Therefore, we set $n_n=2$ for V_1 in this extended bond-counting model. (This is somehow arbitrary but to state that six new bonds are built in the monovacancy would not describe the bonding situation correctly. Therefore, we count distances less or equal 2.8 Å as bonds.) For the simple divacancy in each of the two isosceles triangles described above two new bonds are generated, that is, a total of four new bonds. The divacancy can be considered as a chain of two vacancies; it follows that at each end of a vacancy chain two new bonds are built. The vacancy sites not at the end of the chain have at two nearest-neighbor sites another vacancy and at the other two nearest-neighbor sites they have two atoms from the surrounding crystal. These latter two atoms built one new bond per vacancy. That is, the trivacancy exhibits five new bonds and an open nonbranching chain of *n* vacancies exhibits $2+n$ new bonds. As in the simple bond-counting model this dependency changes if the vacancies form a closed ring. All vacancy sites in a single closed ring have at two of their nearest-neighbor sites another vacancy and at the two other nearest-neighbor sites there are atoms from the surrounding crystal, which rearrange to form a new bond; therefore, a single ring of *n* vacancies exhibits *n* new bonds. Examples of a single ring are the hexagonal ring V_6 (atoms 1–6 in Fig. 1 removed) (Fig. 3 and Table I) and V_8 (atoms 1, 2, 4–6 and 8–10 in Fig. 1 removed) (Table II).

If the vacancies form a network of sixfold rings, which share some vacancy sites, like the vacancy structure V_{10} displayed in Fig. 4(a) or V_{14} displayed in Fig. 6(a), the number of new bonds is fixed at $n_n=6$. This is because these structures introduce vacancy sites, which have at three of their nearest-neighbor sites vacancies and the atoms in the surrounding crystal sitting on the fourth-nearest-neighbor site cannot form a new bond to a next-nearest neighbor. The ring vacancy V_{10} has four of these vacancy sites with three nearest-neighbor vacancy sites and the ring vacancy V_{14} has eight of them. Adding a vacancy next to V_6, V_{10}, or V_{14}, defined by Fig. 1, breaks one of the formerly formed bonds and creates one new bond. Therefore, the number of new bonds equals six for $V_6, V_7, V_{10}, V_{11}, V_{14}$, and V_{15}. Because the new bonds are weaker than the bonds in the ideal crystal and because the formation of the new bonds is accompanied by the weakening of some of the ideal tetrahedral bonds, we add for each new bond an energy of $0.4E_b$ to the energy of a vacancy cluster in the extended bond-counting model. This value yields the best agreement with the SCC-DFTB results.

[1] W. Fuhs, U. Holzhauer, S. Mantl, F.W. Richter, and R. Sturm, Phys. Status Solidi B **89**, 69 (1978).

[2] Motoko-Kwete, D. Segers, M. Dorikens, L. Dorikens-Vanpraet, P. Clauws, and I. Lemanhieu, Appl. Phys. A: Solids Surf. **49**, 659 (1989).

[3] P. Mascher, S. Dannefaer, and D. Kerr, Phys. Rev. B **40**, 11 764 (1989).

[4] A. Polity, F. Börner, S. Huth, S. Eichler, and R. Krause-Rehberg, Phys. Rev. B **58**, 10 363 (1998).

[5] Young-Hoon Lee and James W. Corbett, Phys. Rev. B **8**, 2810 (1973).

[6] Young-Hoon Lee and James W. Corbett, Phys. Rev. B **9**, 4351 (1974).

[7] M. Huang, Y. Wang, J. Yang, Y. He, Y. Guo, and C. Liu, Mater. Sci. Forum **105-110**, 1071 (1992).

[8] R. Krause-Rehberg, M. Brohl, H.S. Leipner, Th. Drost, A. Polity, U. Beyer, and H. Alexander, Phys. Rev. B **47**, 13 266 (1993).

[9] T.Y. Tan, P. Plekhanov, and U.M. Gösele, Appl. Phys. Lett. **70**, 1715 (1997).

[10] D.J. Chadi and K.J. Chang, Phys. Rev. B **38**, 1523 (1988).

[11] M. Lannoo, Mater. Sci. Eng., B **22**, 1 (1993).

[12] H. Seong and L.J. Lewis, Phys. Rev. B **53**, 9791 (1996).

[13] J.L. Hastings, S.K. Estreicher, and P.A. Fedders, Phys. Rev. B **56**, 10 215 (1997).

[14] M.J. Puska, S. Pöykkö, M. Pesola, and R.M. Nieminen, Phys. Rev. B **58**, 1318 (1998).

[15] S. Ögüt and J.R. Chelikowsky, Phys. Rev. Lett. **83**, 3852 (1999).

[16] A. Bongiorno, L. Colombo, and T. Diaz de la Rubia, Europhys. Lett. **43**, 695 (1998).

[17] Th. Frauenheim, F. Weich, Th. Köhler, S. Uhlmann, D. Porezag, and G. Seifert, Phys. Rev. B **52**, 11 492 (1995).

[18] M. Elstner, D. Porezag, G. Jungnickel, J. Elsner, M. Haugk, Th. Frauenheim, S. Shuhai, and G. Seifert, Phys. Rev. B **58**, 7260 (1998).

[19] R. Krause-Rehberg and H. S. Leipner, *Defects in Semiconductors*, 1st ed. (Springer-Verlag, Berlin, 1999).

[20] Zhu Shenyun, Li Anli, Li Donghong, Huang Hanchen, Zheng Shengnan, Du Hongshan, Ding Honglin, Gou Zhenhui, and T. Iwata, Mater. Sci. Forum **175-178**, 609 (1995).

[21] Motoko-Kwete, D. Segers, M. Dorikens, L. Dorikens-Vanpraet, P. Clauws, and I. Lemanhieu, in *Positron Annihilation Proccedings of the ICPA-8 Gent, 1989*, edited by L. Dorikens-Vanpraet, M. Dorikens, and D. Segers (World Scientific, Singapore, 1989), pp. 687–689.

[22] B. Somieski, T.E.M. Staab, and R. Krause-Rehberg, Nucl. Instrum. Methods Phys. Res. A **381**, 128 (1996).

[23] T.E.M. Staab, B. Somieski, and R. Krause-Rehberg, Nucl. Instrum. Methods Phys. Res. A **381**, 141 (1996).

[24] M. Brohl, C. Kisielowski, and H. Alexander, Appl. Phys. Lett. **50**, 1733 (1987).

[25] S. Dannefaer, D. Kerr, and B.G. Hogg, J. Appl. Phys. **54**, 155 (1983).

[26] C. G. Hübner, Ph.D. thesis, Martin-Luther Universität Halle-Wittenberg, Halle/Saale, Germany, 1998.

[27] A. Sieck, D. Porezag, Th. Frauenheim, M.R. Pederson, and K. Jackson, Phys. Rev. A **56**, 4890 (1997).

[28] M. Haugk, J. Elsner, Th. Heine, Th. Frauenheim, and G. Seifert, Comput. Mater. Sci. **13**, 239 (1999).

[29] M.J. Puska and R.M. Nieminen, J. Phys. F: Met. Phys. **13**, 333 (1983).

[30] M.J. Puska, S. Mäkinen, M. Manninen, and R.M. Nieminen, Phys. Rev. B **39**, 7666 (1989).

[31] E. Bornonski and R.M. Nieminen, Phys. Rev. B **34**, 3820 (1986).

[32] M. Saito and A. Oshiyama, Phys. Rev. B **53**, 7810 (1996).
[33] T.E.M. Staab, M. Haugk, Th. Frauenheim, and H.S. Leipner, Phys. Rev. Lett. **83**, 5519 (1999).
[34] A. Antonelli, E. Kaxiras, and D.J. Chadi, Phys. Rev. Lett. **81**, 2088 (1998).
[35] M. Pesola, J. von Boehm, S. Pöykkö, and R.M. Nieminen, Phys. Rev. B **58**, 1106 (1998).
[36] R. M. Nieminen and M. J. Puska, in *Properties of Crystalline Silicon*, edited by R. Hull, EMIS Datareviews Series No. 20 (EMIS, London, 1999), p. 309.
[37] E.G. Song, E. Kim, Y.H. Lee, and Y.G. Hwang, Phys. Rev. B **48**, 1486 (1993).
[38] T.E.M. Staab, M.J. Puska, M. Hakala, A. Sieck, M. Haugk, Th. Frauenheim, and H.S. Leipner Mater. Sci. Forum **363-365**, 135 (2001).
[39] S.K. Estreicher, J.L. Hastings, and P.A. Fedders, Appl. Phys. Lett. **70**, 432 (1997).
[40] M.J. Puska and C. Corbel Phys. Rev. B **38**, 9874 (1988).
[41] M. Hakala, M.J. Puska, and R.M. Niemienen, Phys. Rev. B **57**, 7621 (1998).
[42] A. La Magna, S. Coffa, and L. Colombo, Phys. Rev. Lett. **82**, 1720 (1999).